First observation of the $\Lambda_b^0 \to \Lambda_c^+ D_s^- K^+ K^-$ decay and search for pentaquarks in the $\Lambda_c^+ D_s^-$ system

R. Aaij *et al.*[*]
(LHCb Collaboration)

(Received 15 July 2025; accepted 28 August 2025; published 29 September 2025)

The $\Lambda_b^0 \to \Lambda_c^+ D_s^- K^+ K^-$ decay is observed for the first time using the data sample from proton-proton collisions recorded at a center-of-mass energy of 13 TeV with the LHCb detector, corresponding to an integrated luminosity of 6 fb^{-1}. The ratio of branching fraction to that of $\Lambda_b^0 \to \Lambda_c^+ D_s^-$ decays is measured as $0.0141 \pm 0.0019 \pm 0.0012$, where the first uncertainty is statistical and the second systematic. A search for hidden-charm pentaquarks with strangeness is performed in the $\Lambda_c^+ D_s^-$ system. No evidence is found, and upper limits on the production ratio of $P_{c\bar{c}s}(4338)^0$ and $P_{c\bar{c}s}(4459)^0$ pentaquarks relative to the $\Lambda_c^+ D_s^-$ final state are set at the 95% confidence level as 0.12 and 0.20, respectively.

DOI: 10.1103/b28d-z2xc

I. INTRODUCTION

Pentaquarks with minimal quark composition of three quarks plus a quark-antiquark pair have been predicted since the establishment of the quark model [1]. Hidden-charm pentaquark candidates ($P_{c\bar{c}}^+ = c\bar{c}uud$) were first observed in the $J/\psi p$ system, produced through $\Lambda_b^0 \to J/\psi p K^-$ decays recorded by the LHCb experiment [2–4].[1] A pentaquark candidate ($P_{c\bar{c}s}^0 = c\bar{c}uds$) with strangeness was observed in the $J/\psi\Lambda$ system in $B^- \to J/\psi\Lambda\bar{p}$ decays [5]. Besides, evidence for candidate $P_{c\bar{c}}^+$ and $P_{c\bar{c}s}^0$ resonances was found in the $B_s^0 \to J/\psi p\bar{p}$ decay and $\Xi_b^- \to J/\psi\Lambda K^-$ decay, respectively [6,7]. The $P_{c\bar{c}}^+$ candidates are found near the threshold for the production of $\Sigma_c^+ \bar{D}^{(*)0}$ states, and $P_{c\bar{c}s}^0$ candidates are found close to the threshold of $\Xi_c \bar{D}^{(*)}$ states. Various interpretations, including hadronic molecules [8–12], tightly bound pentaquark states [13–19] and threshold effects [20–23], have been proposed, but their nature remains largely unknown. Measurements in different decay channels are crucial for testing and distinguishing these interpretations [24–26].

Several searches for pentaquarks have been conducted in open-charm final states at LHCb. The prompt production of hidden-charm pentaquark states decaying to $\Sigma_c \bar{D}$ and $\Lambda_c^+ \bar{D}$, as well as doubly charmed pentaquark states decaying to $\Sigma_c D$ and $\Lambda_c^+ D$, have been studied [27]. Additionally, the observation of $\Lambda_b^0 \to \Lambda_c^+ \bar{D}^0 K^-$ and $\Lambda_b^0 \to \Sigma_c^{(*)++} D^{(*)-} K^-$ decays allows for testing pentaquark states in the $\Lambda_c^+ \bar{D}^0$ and $\Sigma_c^{(*)++} D^{(*)-}$ systems, respectively [28,29]. However, no evidence for such states has been found in these studies.

The $\Lambda_b^0 \to \Lambda_c^+ D_s^- K^+ K^-$ decay offers a special opportunity to search for pentaquark candidates in the $\Lambda_c^+ D_s^-$ system, whose leading Feynman diagrams are shown in Fig. 1. In particular, in the $\Lambda_b^0 \to \Lambda_c^+ D_s^- \phi$ process, the phase space of the $\Lambda_c^+ D_s^-$ system extends from 4235 to 4632 MeV,[2] and, thus, encompasses the masses of the two pentaquark candidates $P_{c\bar{c}s}(4338)^0$ and $P_{c\bar{c}s}(4459)^0$, previously observed in the decays $B^- \to J/\psi\Lambda\bar{p}$ and $\Xi_b^- \to J/\psi\Lambda K^-$, respectively. Meanwhile, searches for highly excited Λ_c^+ and D_s^- states, as well as exotic particles in the $\Lambda_c^+\phi$ and $D_s^-\phi$ systems, can also be performed.

In this paper, the first observation of the $\Lambda_b^0 \to \Lambda_c^+ D_s^- K^+ K^-$ decay is reported. The relative branching fraction with respect to the $\Lambda_b^0 \to \Lambda_c^+ D_s^-$ decay is measured, and a search for pentaquark candidates in the $\Lambda_c^+ D_s^-$ system is performed, using proton-proton (pp) collision data at a center-of-mass energy of 13 TeV, corresponding to a luminosity of 6 fb^{-1}, collected by the LHCb experiment between 2015 and 2018. The Cabibbo-favored decay $\Lambda_b^0 \to \Lambda_c^+ D_s^-$ is chosen as the normalization mode for the branching fraction measurement due to its larger statistics and the same parent particle and intermediate states. It also serves as a control mode for applying corrections to simulated samples using a data-driven method.

[*]Full author list given at the end of the article.

[1]Inclusion of charge-conjugate processes is implied throughout.

[2]Natural units with $\hbar = c = 1$ are used throughout.

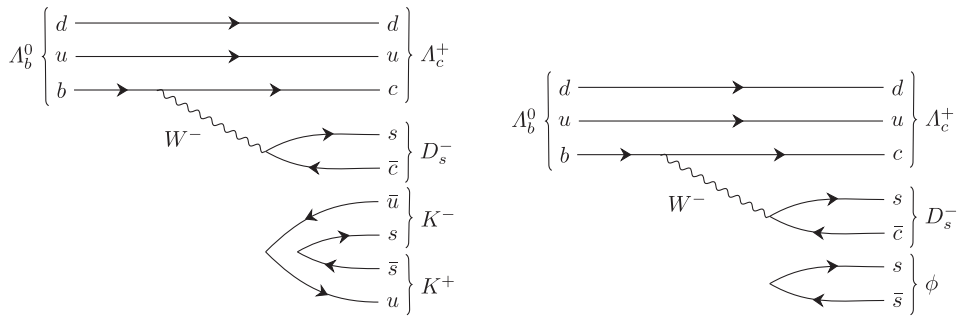

(a) The nonresonant K^+K^- process (b) The ϕ-dominated process

FIG. 1. Tree-level Feynman diagrams of the $\Lambda_b^0 \to \Lambda_c^+ D_s^- K^+ K^-$ decay.

II. DETECTOR AND SIMULATION

The LHCb detector [30,31] is a single-arm forward spectrometer covering the pseudorapidity range $2 < \eta < 5$, designed for the study of particles containing b or c quarks. The detector elements that are particularly relevant to this analysis are: a silicon-strip vertex locator (VELO) surrounding the pp interaction region that allows c and b hadrons to be identified from their characteristically long flight distance; a tracking system that provides a measurement of the momentum, p, of charged particles; and two ring-imaging Cherenkov detectors that are able to discriminate between different species of charged hadrons.

The online event selection is performed by a trigger which consists of a hardware stage followed by a two-level software stage [32]. At the hardware stage, events are required to have a muon with high momentum transverse to the beam, p_{T}, or a hadron, photon, or electron with high transverse energy in the calorimeters. For hadrons, the transverse energy threshold is 3.5 GeV. In the offline selection, the software trigger requires a two-, three-, or four-track secondary vertex with a significant displacement from any primary pp interaction vertex (PV). At least one charged particle must have a $p_{\mathrm{T}} > 1.6$ GeV and be inconsistent with originating from a PV. A multivariate algorithm [33,34] is used for the identification of secondary vertices consistent with the decay of a Λ_b^0 hadron.

Simulation is required to model the effects of the detector acceptance and the imposed selection requirements. In the simulation, pp collisions are generated using PYTHIA [35,36] with a specific LHCb configuration [37]. Decays of unstable particles are described by EvtGen [38], in which final-state radiation is generated using PHOTOS [39]. The interaction of the generated particles with the detector, and its response, are implemented using the Geant4 toolkit [40] as described in Ref. [41].

The kinematic distribution of Λ_b^0 baryons is not perfectly modeled in the simulation framework. Differences in p_{T} and η distributions between data and simulated events for both signal and normalization modes are corrected using a data-driven approach. Additionally, the simulated decay amplitudes for $\Lambda_c^+ \to pK^-\pi^+$ and $D_s^- \to K^+K^-\pi^-$ decays do not fully match those observed in data, and corrections for the Λ_c^+ and D_s^- decay amplitudes are derived from $\Lambda_b^0 \to \Lambda_c^+ D_s^-$ decays by comparing their Dalitz plots in data and simulation.

III. DATASET AND SELECTION

The data undergo additional filtering in an offline selection process. Candidates consistent with the exclusive decays $\Lambda_b^0 \to \Lambda_c^+ D_s^- K^+ K^-$ or $\Lambda_b^0 \to \Lambda_c^+ D_s^-$ are retained, where the Λ_c^+ baryon decays to $p\,K^-\,\pi^+$ and the D_s^- meson decays to $K^+K^-\pi^-$. The selection requires tracks with hits in at least the VELO and the tracking stations downstream of the magnet [42]. A further selection is applied, requiring that each final-state track has $p_{\mathrm{T}} > 100$ MeV and good track-fit quality and that the Λ_b^0 baryon has a significant displacement of its decay vertex from any PV. Intermediate charmed hadrons are selected using the quality of their decay-vertex fit (χ^2_{vtx}), the displacement of the decay vertex from the associated PV, and the angle between the reconstructed momentum direction and the flight direction determined from the origin and the decay vertices (DIRA). Even though the Λ_c^+ decay produces protons with higher momentum that could be cleanly reconstructed and identified, the shorter lifetime compared to that of the D_s^- meson complicates the suppression of background contributions in the decay $\Lambda_c^+ \to pK^-\pi^+$. Additional kinematic and topological criteria are employed to address this issue, based on the sum of p_{T} of Λ_c^+ decay products and the distance of closest approach of these decay products. Consequently, the $\Lambda_c^+ \to pK^-\pi^+$ decay is selected using a gradient-boosted decision tree (BDT) classifier [43,44] which is trained and validated with $\Lambda_b^0 \to \Lambda_c^+\pi^-$ data [28,45].

The Λ_b^0 baryon is reconstructed by combining a Λ_c^+ baryon with a D_s^- meson for the control mode and together with two additional kaon tracks for the signal mode. Kinematical and topological selections are applied, including p_{T}, χ^2_{vtx}, DIRA, χ^2_{IP} (defined as the difference in the vertex fit χ^2 of a primary vertex reconstructed with and without the Λ_b^0 candidate), and the quality of the kinematic

fit, which requires the Λ_b^0 to originate from its associated primary vertex [46]. The particle identification (PID) probability of each final-state track, derived from a neural network combining PID information across the detector, is used to suppress topologically similar backgrounds [31]. To enhance the mass resolution, the mass of the Λ_b^0 baryon for both signal and normalization modes is derived from a global decay chain fit with a Kalman filter [46], which constrains the Λ_b^0 to originate from its associated PV and the Λ_c^+ and D_s^- masses to their known values [47].

A dedicated BDT classifier is trained using simulated events as the signal proxy and the upper sideband data $[m(\Lambda_c^+ D_s^- K^+ K^-) \in [5700, 6200]$ MeV] as the background proxy, to suppress combinatorial background in Λ_b^0 decays. The BDT employs the AdaBoost algorithm [44,48] to enhance its performance. Several kinematical variables, PID variables, and the vertex-fit quality are used as discriminating features. The BDT output selection criterion is chosen as in Ref. [5] by maximizing the figure of merit $S^2/(S+B)^{3/2}$ to obtain both high signal purity and significance, where S and B are the signal and background yields, respectively, in a region of ± 12 MeV around the known Λ_b^0 mass. To avoid a possible bias due to fluctuations of the signal yield, S is determined from a fit to the $m(\Lambda_c^+ D_s^- K^+ K^-)$ distribution in data selected with a looser BDT requirement and then multiplied by the BDT efficiency derived from simulated samples. The determination of B is obtained by fitting the Λ_b^0 mass distribution within $m(\Lambda_c^+ D_s^- K^+ K^-) \in [5540, 5590] \cup [5700, 5950]$ MeV and subsequently extrapolating linearly into the signal region. An independent BDT classifier is trained to select normalization mode candidates using a similar strategy and is optimized with the same figure of merit.

Candidates with an opening angle between any track pair smaller than 0.5 mrad are rejected, removing artifacts from wrong matching of track segments reconstructed within the tracking stations and the VELO.

Some events passing all selection criteria contain multiple candidates. In such cases, a single candidate is retained at random. The potential bias arising from this random selection is subsequently evaluated as a systematic uncertainty.

IV. SIGNAL EXTRACTION

The yield of the $\Lambda_b^0 \to \Lambda_c^+ D_s^- K^+ K^-$ signal decay is determined through an unbinned maximum-likelihood fit to the $m(\Lambda_c^+ D_s^- K^+ K^-)$ mass distribution. The Λ_b^0 signal is modeled using a linear combination of a Crystal Ball distribution [49] and a Johnson S_U distribution [50]. These distributions share identical peak positions and widths, which are floated in the fit, while the tail parameters and the relative intensity are fixed to values obtained from fits to simulated data. The combinatorial background is described by a first-order Chebyshev polynomial.

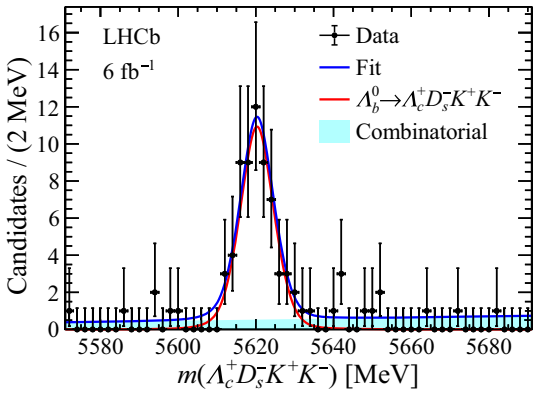

FIG. 2. Mass distribution of Λ_b^0 candidates reconstructed using the $\Lambda_b^0 \to \Lambda_c^+ D_s^- K^+ K^-$ decays, with the fit result also shown.

The fit result, shown in Fig. 2, yields 61 ± 8 signal $\Lambda_b^0 \to \Lambda_c^+ D_s^- K^+ K^-$ decays, where the uncertainty is statistical only. The performance of the maximum-likelihood fit is validated by generating and fitting 500 pseudoexperiments using the baseline model, with no significant bias observed for the signal decay mode.

The contribution from the $\Lambda_b^0 \to \Lambda_c^+ D_s^- \phi$ process is determined by fitting the background-subtracted $m(K^+K^-)$ distribution in $\Lambda_b^0 \to \Lambda_c^+ D_s^- K^+ K^-$ decays, where backgrounds are subtracted using the sPlot technique [51]. The ϕ signal is modeled with a relativistic Breit-Wigner distribution, while the remaining non-ϕ component is described by an empirical function. As is illustrated in Fig. 3, the ϕ component is found to be significantly more prominent than the non-ϕ contribution. Furthermore, analysis of the background-subtracted $\Lambda_c^+ \phi$ and $D_s^- \phi$ invariant mass distributions shows no evidence for resonant states.

The yield of the normalization mode $\Lambda_b^0 \to \Lambda_c^+ D_s^-$ is determined through a fit to the $m(\Lambda_c^+ D_s^-)$ distribution. Both the signal and background components for the normalization decay are modeled in the same manner as for the signal decay. The fitted yield for the $\Lambda_b^0 \to \Lambda_c^+ D_s^-$ decay mode is

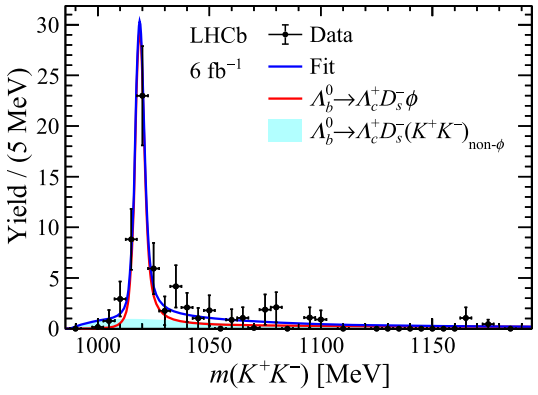

FIG. 3. Distribution of $m(K^+K^-)$ for background-subtracted $\Lambda_b^0 \to \Lambda_c^+ D_s^- K^+ K^-$ decays with the fit result also shown.

determined to be $(31.27 \pm 0.19) \times 10^3$, where the uncertainty is statistical only. The same validation procedure used for the signal decay mode is applied to the normalization decay mode, resulting in a relative yield shift of 0.2%, which is assigned as a systematic uncertainty.

V. RELATIVE BRANCHING FRACTION

In order to determine the ratio of branching fractions, the efficiencies for the signal and normalization channels are estimated from corrected simulated samples, including the effects of detector acceptance, triggers, reconstruction, and offline selection. Since the intermediate states in $\Lambda_b^0 \to \Lambda_c^+ D_s^- K^+ K^-$ decays are not perfectly modeled in the simulation, the yield of the signal mode is corrected by considering a per-event efficiency,

$$n_{\rm corr} = \sum_i \frac{s\mathcal{W}_i}{\epsilon(m_i^2(\Lambda_c^+ K^+ K^-), m_i^2(D_s^- K^+ K^-))}, \quad (1)$$

where $n_{\rm corr}$ is the efficiency-corrected yield, $s\mathcal{W}_i$ is the per-event weight used to subtract background, and $\epsilon(m_i^2(\Lambda_c^+ K^+ K^-), m_i^2(D_s^- K^+ K^-))$ is the mass-dependent per-event efficiency.

The efficiency-corrected yield for the two-body decay $\Lambda_b^0 \to \Lambda_c^+ D_s^-$ can be simplified as $n(\Lambda_b^0 \to \Lambda_c^+ D_s^-)/\epsilon(\Lambda_b^0 \to \Lambda_c^+ D_s^-)$, where n and ϵ represent the yield and efficiency of the normalization decay mode, respectively. Using these quantities, the ratio of branching fractions is calculated as

$$\frac{\mathcal{B}(\Lambda_b^0 \to \Lambda_c^+ D_s^- K^+ K^-)}{\mathcal{B}(\Lambda_b^0 \to \Lambda_c^+ D_s^-)} = \frac{n_{\rm corr}(\Lambda_b^0 \to \Lambda_c^+ D_s^- K^+ K^-)}{n_{\rm corr}(\Lambda_b^0 \to \Lambda_c^+ D_s^-)}, \quad (2)$$

yielding a value of 0.0141 ± 0.0019, where the uncertainty is statistical only.

VI. SYSTEMATIC UNCERTAINTIES

The signal decay $\Lambda_b^0 \to \Lambda_c^+ D_s^- K^+ K^-$ includes two additional kaon tracks compared to the normalization $\Lambda_b^0 \to \Lambda_c^+ D_s^-$ decay. The modeling of track reconstruction efficiency in the simulation introduces a systematic uncertainty of 1.36% for each extra kaon, arising from the imperfect simulation of hadronic interactions with the detector material [52].

Imperfections in the estimation of the hardware trigger efficiencies are present in both signal mode and normalization mode. A data-driven approach [32] is used to calculate the correction factor in bins of the maximum $p_{\rm T}$ of the final-state tracks. In the baseline measurement, independent correction tables derived from data for the corresponding decays are applied to the $\Lambda_b^0 \to \Lambda_c^+ D_s^- K^+ K^-$ and $\Lambda_b^0 \to \Lambda_c^+ D_s^-$ simulations. Systematic uncertainties in these corrections are estimated by either using a single correction table for both decay modes or by applying the correction factors derived from $\Lambda_b^0 \to \Lambda_c^+ D_s^- K^+ K^-$ and $\Lambda_b^0 \to \Lambda_c^+ D_s^-$ decays to the $\Lambda_b^0 \to \Lambda_c^+ D_s^-$ and $\Lambda_b^0 \to \Lambda_c^+ D_s^- K^+ K^-$ simulations, respectively. The largest change in the efficiency ratio between $\Lambda_b^0 \to \Lambda_c^+ D_s^- K^+ K^-$ and $\Lambda_b^0 \to \Lambda_c^+ D_s^-$ decays is 1.6%, which is assigned as the systematic uncertainty due to the hardware trigger efficiency correction.

The simulated PID response is calibrated using control samples and the kernel density estimation method [53,54]. This correction accounts for two sources of uncertainty: one arising from the kernel density estimation algorithm and the other from the finite size of the calibration samples. To assess the systematic uncertainty, the kernel density estimation template is varied by increasing the kernel width by 50% and by employing a bootstrapping method. The resulting variations in the efficiency ratios are assigned as systematic uncertainties corresponding to each source.

The systematic uncertainties related to the fit models are evaluated with pseudoexperiments generated with the baseline model and fitted with alternative signal and background parametrizations. For the Λ_b^0 signal, an alternative model is used, based on a modified Crystal Ball function with tails on both sides of the peak, while the background model is replaced with an exponential function instead of the Chebyshev polynomial. The yield shift is quantified as the difference between the yield obtained from the baseline fit to data and the mean yield derived from the ensemble of pseudoexperiments. Considering the shifts for both signal and normalization modes, the difference in the signal yield ratio is assigned as the systematic uncertainty.

To account for potential signal loss introduced by the random selection of multiple candidates, the procedure is repeated 500 times with different random seeds, performing a signal yield fit for each iteration. The corresponding systematic uncertainty is evaluated as the difference between the nominal signal yield and the mean of the resulting distribution.

The systematic uncertainty arising from the limited size of the simulated samples is estimated using a Bayesian approach, where the number of selected candidates for the true efficiency in each $(m^2(\Lambda_c^+ K^+ K^-), m^2(D_s^- K^+ K^-))$ bin in Eq. (1) is assumed to be binomially distributed, and the prior probability is chosen as a uniform distribution, both of which are used to determine the posterior probability of the efficiency in actual measurements. The uncertainty on the efficiency table is evaluated independently for each bin and subsequently propagated to the ratio of branching fractions. Additionally, the binning scheme used in the efficiency parametrization is varied, and the largest observed difference in the ratio of branching fractions is assigned as the systematic uncertainty.

To estimate the systematic uncertainty associated with the correction for Λ_c^+ and D_s^- decay amplitudes, the correction is removed from the simulated events. The resulting difference

TABLE I. Summary of relative systematic uncertainties on the relative branching fraction.

Sources	Relative uncertainty (%)
Fit bias	0.2
Tracking efficiency	2.7
Trigger efficiency	1.6
PID correction algorithm	0.6
Signal fit model	0.6
Background fit model	0.3
Multiple candidates	2.5
Simulated sample sizes	5.3
Binning scheme in $n_{\rm corr}$ calculation	2.3
Correction on Λ_c^+ and D_s^- decay amplitudes	2.0
Total	8.7

in the branching fraction ratio is assigned as a systematic uncertainty. The magnitude of this difference depends on the size of the simulated samples, making this uncertainty fully correlated with the uncertainty arising from the limited size of the simulated samples.

The summary of the systematic uncertainties is presented in Table I, where correlations among different sources are taken into account when determining the total uncertainty. The systematic uncertainty on the relative branching fraction measurement is found to be smaller than the statistical uncertainty.

VII. UPPER LIMITS ON THE $P^0_{c\bar{c}s}$ PRODUCTION RATE

A search for a $P^0_{c\bar{c}s} \to \Lambda_c^+ D_s^-$ contribution to the $\Lambda_b^0 \to \Lambda_c^+ D_s^- K^+ K^-$ decay is performed by inspecting the mass distribution of $\Lambda_c^+ D_s^-$ where the background is subtracted with the sPlot technique. The mass $m(\Lambda_c^+ D_s^-)$ is computed from a kinematic fit [46] which requires the Λ_b^0 baryon to originate from its associated primary vertex and constrains the Λ_c^+, D_s^-, and Λ_b^0 hadrons to their known masses [47]. A weighted unbinned maximum-likelihood fit [55] is applied to the $m(\Lambda_c^+ D_s^-)$ distribution, where the data are described as the incoherent sum of $P^0_{c\bar{c}s} \to \Lambda_c^+ D_s^-$ decays and a nonresonant Λ_c^+ D_s^- contribution. The $P^0_{c\bar{c}s}$ resonance is modeled using a relativistic Breit-Wigner function [47,56], with parameters for $P_{c\bar{c}s}(4338)^0$ and $P_{c\bar{c}s}(4459)^0$ resonances obtained from Refs. [5] and [7], respectively. The line shape is described in detail in the Appendix. It is subsequently convolved with a Gaussian resolution function whose shape parameters are determined from simulation. The contribution from $\Lambda_b^0 \to \Lambda_c^+ D_s^- K^+ K^-$ decays with a nonresonant Λ_c^+ D_s^- system is modeled using simulated $\Lambda_b^0 \to \Lambda_c^+ D_s^- \phi$ decays generated uniformly over the phase space. The fit projections for $P_{c\bar{c}s}(4338)^0$ and $P_{c\bar{c}s}(4459)^0$ resonances are shown in Fig. 4. Both fits yield significances below 2σ, showing no significant pentaquark contributions in the Λ_c^+ D_s^- system.

Defining the relative $P^0_{c\bar{c}s}$ contribution as

$$\mathcal{R}_{P^0_{c\bar{c}s}} \equiv \frac{\mathcal{B}(\Lambda_b^0 \to P_{c\bar{c}s} K^+ K^-)}{\mathcal{B}(\Lambda_b^0 \to \Lambda_c^+ D_s^- K^+ K^-)} \cdot \mathcal{B}(P^0_{c\bar{c}s} \to \Lambda_c^+ D_s^-), \quad (3)$$

the upper limits on the production rates are determined to be $\mathcal{R}_{P_{c\bar{c}s}(4338)^0} < 0.12(0.10)$ and $\mathcal{R}_{P_{c\bar{c}s}(4459)^0} < 0.20(0.17)$ at the 95% (90%) confidence level. These limits are derived by integrating the probability distribution of $\mathcal{R}_{P^0_{c\bar{c}s}}$, ensuring that the integral up to the upper limit equals 0.95 (0.90) times the total integral [57]. Systematic uncertainties associated with the modeling of the pentaquark line shape and of the nonresonant contribution are found to have negligible impact on the measured $\mathcal{R}_{P^0_{c\bar{c}s}}$ values.

VIII. CONCLUSION

The $\Lambda_b^0 \to \Lambda_c^+ D_s^- K^+ K^-$ decay has been observed for the first time, and the branching fraction relative to the $\Lambda_b^0 \to \Lambda_c^+ D_s^-$ decay is measured to be

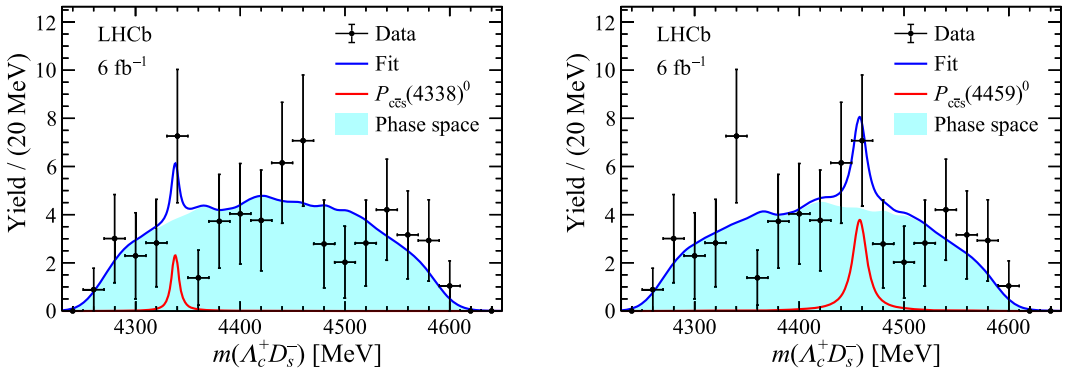

FIG. 4. Distribution of $m(\Lambda_c^+ D_s^-)$ for background-subtracted $\Lambda_b^0 \to \Lambda_c^+ D_s^- K^+ K^-$ decays with the fit result also shown. The red line shows the contribution from the (left) $P_{c\bar{c}s}(4338)^0$ and (right) $P_{c\bar{c}s}(4459)^0$ state, while the cyan fill represents the phase-space distribution of the $\Lambda_b^0 \to \Lambda_c^+ D_s^- \phi$ decay.

$$\frac{\mathcal{B}(\Lambda_b^0 \to \Lambda_c^+ D_s^- K^+ K^-)}{\mathcal{B}(\Lambda_b^0 \to \Lambda_c^+ D_s^-)} = 0.0141 \pm 0.0019 \pm 0.0012,$$

where the first uncertainty is statistical and the second is systematic.

No significant pentaquark signal was identified in the $m(\Lambda_c^+ D_s^-)$ mass spectrum. With only 61 candidates detected, the sample size is insufficient to perform an amplitude analysis. Upper limits on the fit fractions of $P_{c\bar{c}s}(4338)^0$ and $P_{c\bar{c}s}(4459)^0$ decaying to the $\Lambda_c^+ D_s^-$ final state are therefore set at 0.12(0.10) and 0.20(0.17), respectively, at the 95% (90%) confidence level. Furthermore, no evidence for excited charmed hadrons or exotic states is found in the $\Lambda_c^+\phi$ or $D_s^-\phi$ mass distributions.

It is anticipated that this statistical limitation will be surmounted with the ongoing higher-luminosity data acquisition, facilitated by the upgraded LHCb detector. The larger data samples due to increased luminosity and trigger efficiency are expected to enable a more comprehensive analysis [58,59]. Future larger datasets will allow for a full amplitude analysis that can take into account the Λ_c^+ polarization [60,61] and ϕ decay degrees of freedom, which will contribute to the properties of the strange pentaquarks with hidden charm.

ACKNOWLEDGMENTS

We express our gratitude to our colleagues in the CERN accelerator departments for the excellent performance of the LHC. We thank the technical and administrative staff at the LHCb institutes. We acknowledge support from CERN and from the national agencies: ARC (Australia); CAPES, CNPq, FAPERJ, and FINEP (Brazil); MOST and NSFC (China); CNRS/IN2P3 (France); BMBF, DFG, and MPG (Germany); INFN (Italy); NWO (Netherlands); MNiSW and NCN (Poland); MCID/IFA (Romania); MICIU and AEI (Spain); SNSF and SER (Switzerland); NASU (Ukraine); STFC (United Kingdom); DOE NP and NSF (USA). We acknowledge the computing resources that are provided by ARDC (Australia), CBPF (Brazil), CERN, IHEP and LZU (China), IN2P3 (France), KIT and DESY (Germany), INFN (Italy), SURF (Netherlands), Polish WLCG (Poland), IFIN-HH (Romania), PIC (Spain), CSCS (Switzerland), and GridPP (United Kingdom). We are indebted to the communities behind the multiple open-source software packages on which we depend. Individual groups or members have received support from Key Research Program of Frontier Sciences of CAS, CAS PIFI, CAS CCEPP, Fundamental Research Funds for the Central Universities, and Sci. & Tech. Program of Guangzhou (China); Minciencias (Colombia); EPLANET, Marie Skłodowska-Curie Actions, ERC, and NextGenerationEU (European Union); A*MIDEX, ANR, IPhU and Labex P2IO, and Région Auvergne-Rhône-Alpes (France); Alexander-von-Humboldt Foundation (Germany); ICSC (Italy); Severo Ochoa and María de Maeztu Units of Excellence, GVA, XuntaGal, GENCAT, InTalent-Inditex and Prog. Atracción Talento CM (Spain); SRC (Sweden); the Leverhulme Trust, the Royal Society and UKRI (United Kingdom).

DATA AVAILABILITY

The data that support the findings of this article are openly available [62].

APPENDIX: LINE SHAPE OF THE PENTAQUARK

For modeling the pentaquark resonances, the Breit-Wigner propagator is employed, expressed as

$$\mathrm{BW}(m|m_0,\Gamma_0) = \frac{1}{m_0^2 - m^2 - i m_0 \Gamma(m)}, \tag{A1}$$

where m represents the mass of the Λ_c^+ D_s^+ system, m_0 represents the mass of the pentaquark taken from Ref. [47], and $\Gamma(m)$ is the mass-dependent width. Given that the only known decay channel for $P_{c\bar{c}s}(4338)^0$ and $P_{c\bar{c}s}(4459)^0$ is $J/\psi\Lambda$, the energy-dependent width is calculated based on the $J/\psi\Lambda$ system. Under the S-wave assumption, the $\Gamma(m)$ is simplified as

$$\Gamma(m) = \Gamma_0 \cdot \frac{q(m, m_{J/\psi}, m_\Lambda)}{q(m_0, m_{J/\psi}, m_\Lambda)} \cdot \frac{m_0}{m}, \tag{A2}$$

where Γ_0 is the natural width of the pentaquark state, $q(m, m_1, m_2)$ is the breakup momentum calculated by

$$q(m, m_1, m_2) = \frac{\sqrt{[m^2 - (m_1 + m_2)^2][m^2 - (m_1 - m_2)^2]}}{2m}, \tag{A3}$$

and m_1 and m_2 are the masses of the two decay products.

The pentaquark line shape $\mathcal{P}_{\mathrm{sig}}(m|m_0,\Gamma_0)$ is then obtained by incorporating a phase-space factor $\rho(m) = p_{\Lambda_b^0} q_{P_{c\bar{c}s}}$ and a normalization constant $\mathcal{N}$, derived as

$$\mathcal{P}_{\mathrm{sig}}(m|m_0,\Gamma_0) = \frac{|\mathrm{BW}(m|m_0,\Gamma_0)|^2 \cdot p_{\Lambda_b^0}(m) q_{P_{c\bar{c}s}}(m)}{\mathcal{N}}, \tag{A4}$$

where $q_{P_{c\bar{c}s}}(m) = q(m, m_{\Lambda_c^+}, m_{D_s^-})$ represents the momentum of Λ_c^+ in the pentaquark rest frame and $p_{\Lambda_b^0}(m) = q(m_{\Lambda_b^0}, m, m_\phi)$ denotes the momentum of the pentaquark in the Λ_b^0 rest frame.

The normalized background line shape $\mathcal{P}_{\rm bkg}(m)$ is derived from the phase-space simulation [54], where the kinematics of the Λ_b^0 hadron and decay amplitudes of the Λ_c^+ and D_s^+ hadrons are corrected to match the data.

Finally, the total fit model is constructed by adding the signal and the background components, expressed as

$$\mathcal{P}(m|m_0,\Gamma_0) = \mathcal{R}_{P^0_{c\bar{c}s}}\mathcal{P}_{\rm sig}(m|m_0,\Gamma_0) + (1-\mathcal{R}_{P^0_{c\bar{c}s}})\mathcal{P}_{\rm bkg}(m). \tag{A5}$$

[1] M. Gell-Mann, A schematic model of baryons and mesons, Phys. Lett. **8**, 214 (1964); G. Zweig, An SU_3 model for strong interaction symmetry and its breaking; Version 1 Report No. CERN-TH-401, CERN, Geneva, 1964.

[2] R. Aaij *et al.* (LHCb Collaboration), Observation of $J/\psi p$ resonances consistent with pentaquark states in $\Lambda_b^0 \to J/\psi p K^-$ decays, Phys. Rev. Lett. **115**, 072001 (2015).

[3] R. Aaij *et al.* (LHCb Collaboration), Model-independent evidence for $J/\psi p$ contributions to $\Lambda_b^0 \to J/\psi p K^-$ decays, Phys. Rev. Lett. **117**, 082002 (2016).

[4] R. Aaij *et al.* (LHCb Collaboration), Observation of a narrow pentaquark state, $P_c(4312)^+$, and of two-peak structure of the $P_c(4450)^+$, Phys. Rev. Lett. **122**, 222001 (2019).

[5] R. Aaij *et al.* (LHCb Collaboration), Observation of a $J/\psi\Lambda$ resonance consistent with a strange pentaquark candidate in $B^- \to J/\psi\Lambda\bar{p}$ decays, Phys. Rev. Lett. **131**, 031901 (2023).

[6] R. Aaij *et al.* (LHCb Collaboration), Evidence for a new structure in the $J/\psi p$ and $J/\psi\bar{p}$ systems in $B_s^0 \to J/\psi p\bar{p}$ decays, Phys. Rev. Lett. **128**, 062001 (2022).

[7] R. Aaij *et al.* (LHCb Collaboration), Evidence of a $J/\psi\Lambda$ structure and observation of excited Ξ^- states in the $\Xi_b^- \to J/\psi\Lambda K^-$ decay, Sci. Bull. **66**, 1278 (2021).

[8] J.-J. Wu, R. Molina, E. Oset, and B. S. Zou, Prediction of narrow N^* and Λ^* resonances with hidden charm above 4 GeV, Phys. Rev. Lett. **105**, 232001 (2010).

[9] J.-J. Wu, R. Molina, E. Oset, and B. S. Zou, Dynamically generated N^* and Λ^* resonances in the hidden charm sector around 4.3 GeV, Phys. Rev. C **84**, 015202 (2011).

[10] Z.-C. Yang, Z.-F. Sun, J. He, X. Liu, and S.-L. Zhu, The possible hidden-charm molecular baryons composed of anti-charmed meson and charmed baryon, Chin. Phys. C **36**, 6 (2012).

[11] X.-K. Dong, F.-K. Guo, and B.-S. Zou, A survey of heavy-antiheavy hadronic molecules, Prog. Phys. **41**, 65 (2021).

[12] F.-K. Guo, C. Hanhart, U.-G. Meißner, Q. Wang, Q. Zhao, and B.-S. Zou, Hadronic molecules, Rev. Mod. Phys. **90**, 015004 (2018); **94**, 029901(E) (2022).

[13] S. G. Yuan, K. W. Wei, J. He, H. S. Xu, and B. S. Zou, Study of $qqqc\bar{c}$ five quark system with three kinds of quark-quark hyperfine interaction, Eur. Phys. J. A **48**, 61 (2012).

[14] L. Maiani, A. D. Polosa, and V. Riquer, The new pentaquarks in the diquark model, Phys. Lett. B **749**, 289 (2015).

[15] R. F. Lebed, The pentaquark candidates in the dynamical diquark picture, Phys. Lett. D **749**, 454 (2015).

[16] G.-N. Li, X.-G. He, and M. He, Some predictions of diquark model for hidden charm pentaquark discovered at the LHCb, J. High Energy Phys. 12 (2015) 128.

[17] A. Esposito, A. Pilloni, and A. D. Polosa, Multiquark resonances, Phys. Rep. **668**, 1 (2017).

[18] J.-M. Richard, Exotic hadrons: Review and perspectives, Few Body Syst. **57**, 1185 (2016).

[19] R. Zhu and C.-F. Qiao, Pentaquark states in a diquark–triquark model, Phys. Lett. B **756**, 259 (2016).

[20] F.-K. Guo, U.-G. Meißner, W. Wang, and Z. Yang, How to reveal the exotic nature of the $P_c(4450)$, Phys. Rev. D **92**, 071502 (2015).

[21] X.-H. Liu, Q. Wang, and Q. Zhao, Understanding the newly observed heavy pentaquark candidates, Phys. Lett. B **757**, 231 (2016).

[22] M. Bayar, F. Aceti, F.-K. Guo, and E. Oset, A discussion on triangle singularities in the $\Lambda_b \to J/\psi K^- p$ reaction, Phys. Rev. D **94**, 074039 (2016).

[23] F.-K. Guo, X.-H. Liu, and S. Sakai, Threshold cusps and triangle singularities in hadronic reactions, Prog. Part. Nucl. Phys. **112**, 103757 (2020).

[24] H.-X. Chen, W. Chen, X. Liu, and S.-L. Zhu, The hidden-charm pentaquark and tetraquark states, Phys. Rep. **639**, 1 (2016).

[25] Y. Dong, A. Faessler, and V. E. Lyubovitskij, Description of heavy exotic resonances as molecular states using phenomenological Lagrangians, Prog. Part. Nucl. Phys. **94**, 282 (2017).

[26] S. L. Olsen, T. Skwarnicki, and D. Zieminska, Nonstandard heavy mesons and baryons: Experimental evidence, Rev. Mod. Phys. **90**, 015003 (2018).

[27] R. Aaij *et al.* (LHCb Collaboration), Search for prompt production of pentaquarks in open charm hadron final states, Phys. Rev. D **110**, 032001 (2024).

[28] R. Aaij *et al.* (LHCb Collaboration), Observation of $\Lambda_b^0 \to \Lambda_c^+ \bar{D}^{(*)0} K^-$ and $\Lambda_b^0 \to \Lambda_c^+ D_s^{*-}$ decays, Eur. Phys. J. C **84**, 575 (2024).

[29] R. Aaij *et al.* (LHCb Collaboration), First observation of $\Lambda_b^0 \to \Sigma_c^{(*)++} D^{(*)-} K^-$ decays, Phys. Rev. D **110**, L031104 (2024).

[30] A. A. Alves Jr. *et al.* (LHCb Collaboration), The LHCb detector at the LHC, J. Instrum. **3**, S08005 (2008).

[31] R. Aaij *et al.* (LHCb Collaboration), LHCb detector performance, Int. J. Mod. Phys. A **30**, 1530022 (2015).

[32] R. Aaij *et al.*, The LHCb trigger and its performance in 2011, J. Instrum. **8**, P04022 (2013).

[33] V. V. Gligorov and M. Williams, Efficient, reliable and fast high-level triggering using a bonsai boosted decision tree, J. Instrum. **8**, P02013 (2013).
[34] T. Likhomanenko, P. Ilten, E. Khairullin, A. Rogozhnikov, A. Ustyuzhanin, and M. Williams, LHCb topological trigger reoptimization, J. Phys. Conf. Ser. **664**, 082025 (2015).
[35] T. Sjöstrand, S. Mrenna, and P. Skands, A brief introduction to PYTHIA8.1, Comput. Phys. Commun. **178**, 852 (2008).
[36] T. Sjöstrand, S. Mrenna, and P. Skands, PYTHIA6.4physics and manual, J. High Energy Phys. 05 (2006) 026.
[37] I. Belyaev *et al.*, Handling of the generation of primary events in Gauss, the LHCb simulation framework, J. Phys. Conf. Ser. **331**, 032047 (2011).
[38] D. J. Lange, The EvtGen particle decay simulation package, Nucl. Instrum. Methods Phys. Res., Sect. A **462**, 152 (2001).
[39] N. Davidson, T. Przedzinski, and Z. Was, PHOTOS interface in C++: Technical and physics documentation, Comput. Phys. Commun. **199**, 86 (2016).
[40] J. Allison *et al.* (Geant4 Collaboration), Geant4 developments and applications, IEEE Trans. Nucl. Sci. **53**, 270 (2006); S. Agostinelli *et al.* (Geant4 Collaboration), Geant4: A simulation toolkit, Nucl. Instrum. Methods Phys. Res., Sect. A **506**, 250 (2003).
[41] M. Clemencic, G. Corti, S. Easo, C. R. Jones, S. Miglioranzi, M. Pappagallo, and P. Robbe, The LHCb simulation application, Gauss: Design, evolution and experience, J. Phys. Conf. Ser. **331**, 032023 (2011).
[42] R. Aaij *et al.* (LHCb Collaboration), Tracking of charged particles with nanosecond lifetimes at LHCb, Eur. Phys. J. C **84**, 761 (2024).
[43] J. H. Friedman, Greedy function approximation: A gradient boosting machine, Ann. Stat. **29**, 1189 (2001).
[44] H. Voss, A. Hoecker, J. Stelzer, and F. Tegenfeldt, TMVA—toolkit for multivariate data analysis with ROOT, Proc. Sci., ACAT2007 (**2007**) 040.
[45] R. Aaij *et al.* (LHCb Collaboration), Study of beauty hadron decays into pairs of charm hadrons, Phys. Rev. Lett. **112**, 202001 (2014).
[46] W. D. Hulsbergen, Decay chain fitting with a Kalman filter, Nucl. Instrum. Methods Phys. Res., Sect. A **552**, 566 (2005).
[47] S. Navas *et al.* (Particle Data Group), Review of particle physics, Phys. Rev. D **110**, 030001 (2024).
[48] Y. Freund and R. E. Schapire, A decision-theoretic generalization of on-line learning and an application to boosting, J. Comput. Syst. Sci. **55**, 119 (1997).
[49] T. Skwarnicki, A study of the radiative cascade transitions between the Upsilon-prime and Upsilon resonances, Ph.D. thesis, Institute of Nuclear Physics, Krakow, 1986 [Report No. DESY-F31-86-02].
[50] N. L. Johnson, Systems of frequency curves generated by methods of translation, Biometrika **36**, 149 (1949).
[51] M. Pivk and F. R. Le Diberder, sPlot: A statistical tool to unfold data distributions, Nucl. Instrum. Methods Phys. Res., Sect. A **555**, 356 (2005).
[52] R. Aaij *et al.* (LHCb Collaboration), Measurement of the track reconstruction efficiency at LHCb, J. Instrum. **10**, P02007 (2015).
[53] L. Anderlini *et al.*, The PIDCalib package, Report No. LHCb-PUB-2016-021, 2016.
[54] K. Cranmer, Kernel estimation in high-energy physics, Comput. Phys. Commun. **136**, 198 (2001).
[55] Y. Xie, sFit: A method for background subtraction in maximum likelihood fit, arXiv:0905.0724.
[56] J. D. Jackson, Remarks on the phenomenological analysis of resonances, Nuovo Cimento **34**, 1644 (1964).
[57] I. V. Narsky, Estimation of upper limits using a Poisson statistic, Nucl. Instrum. Methods Phys. Res., Sect. A **450**, 444 (2000).
[58] LHCb Collaboration, Framework TDR for the LHCb upgrade: Technical design report, Report No. CERN-LHCC-2012-007, 2012.
[59] R. Aaij *et al.* (LHCb Collaboration), The LHCb upgrade I, J. Instrum. **19**, P05065 (2024).
[60] R. Aaij *et al.* (LHCb Collaboration), Amplitude analysis of the $\Lambda_c^+ \to pK^-\pi^+$ decay and Λ_c^+ baryon polarization measurement in semileptonic beauty hadron decays, Phys. Rev. D **108**, 012023 (2023).
[61] R. Aaij *et al.* (LHCb Collaboration), Λ_c^+ polarimetry using the dominant hadronic mode, J. High Energy Phys. 07 (2023) 228.
[62] http://cds.cern.ch/record/2938212

R. Aaij,[38] A. S. W. Abdelmotteleb,[57] C. Abellan Beteta,[51] F. Abudinén,[57] T. Ackernley,[61] A. A. Adefisoye,[69] B. Adeva,[47] M. Adinolfi,[55] P. Adlarson,[85] C. Agapopoulou,[14] C. A. Aidala,[87] Z. Ajaltouni,[11] S. Akar,[11] K. Akiba,[38] P. Albicocco,[28] J. Albrecht,[19,b] R. Aleksiejunas,[80] F. Alessio,[49] Z. Aliouche,[63] P. Alvarez Cartelle,[56] R. Amalric,[16] S. Amato,[3] J. L. Amey,[55] Y. Amhis,[14] L. An,[6] L. Anderlini,[27] M. Andersson,[51] P. Andreola,[51] M. Andreotti,[26] S. Andres Estrada,[84] A. Anelli,[31,49,c] D. Ao,[7] F. Archilli,[37,d] Z Areg,[69] M. Argenton,[26] S. Arguedas Cuendis,[9,49] A. Artamonov,[44] M. Artuso,[69] E. Aslanides,[13] R. Ataíde Da Silva,[50] M. Atzeni,[65] B. Audurier,[12] J. A. Authier,[15] D. Bacher,[64] I. Bachiller Perea,[50] S. Bachmann,[22] M. Bachmayer,[50] J. J. Back,[57] P. Baladron Rodriguez,[47] V. Balagura,[15] A. Balboni,[26] W. Baldini,[26] Z. Baldwin,[78] L. Balzani,[19] H. Bao,[7] J. Baptista de Souza Leite,[61] C. Barbero Pretel,[47,12] M. Barbetti,[27] I. R. Barbosa,[70] R. J. Barlow,[63] M. Barnyakov,[25] S. Barsuk,[14] W. Barter,[59] J. Bartz,[69] S. Bashir,[40] B. Batsukh,[5] P. B. Battista,[14] A. Bay,[50] A. Beck,[65] M. Becker,[19] F. Bedeschi,[35] I. B. Bediaga,[2] N. A. Behling,[19] S. Belin,[47] K. Belous,[44] I. Belov,[29] I. Belyaev,[36] G. Benane,[13] G. Bencivenni,[28] E. Ben-Haim,[16] A. Berezhnoy,[44] R. Bernet,[51] S. Bernet Andres,[46]

A. Bertolin,[33] C. Betancourt,[51] F. Betti,[59] J. Bex,[56] Ia. Bezshyiko,[51] O. Bezshyyko,[86] J. Bhom,[41] M. S. Bieker,[18] N. V. Biesuz,[26] P. Billoir,[16] A. Biolchini,[38] M. Birch,[62] F. C. R. Bishop,[10] A. Bitadze,[63] A. Bizzeti,[27,e] T. Blake,[57,f] F. Blanc,[50] J. E. Blank,[19] S. Blusk,[69] V. Bocharnikov,[44] J. A. Boelhauve,[19] O. Boente Garcia,[15] T. Boettcher,[68] A. Bohare,[59] A. Boldyrev,[44] C. S. Bolognani,[82] R. Bolzonella,[26,g] R. B. Bonacci,[1] N. Bondar,[44,49] A. Bordelius,[49] F. Borgato,[33,49] S. Borghi,[63] M. Borsato,[31,c] J. T. Borsuk,[83] E. Bottalico,[61] S. A. Bouchiba,[50] M. Bovill,[64] T. J. V. Bowcock,[61] A. Boyer,[49] C. Bozzi,[26] J. D. Brandenburg,[88] A. Brea Rodriguez,[50] N. Breer,[19] J. Brodzicka,[41] A. Brossa Gonzalo,[47,a] J. Brown,[61] D. Brundu,[32] E. Buchanan,[59] L. Buonincontri,[33,h] M. Burgos Marcos,[82] A. T. Burke,[63] C. Burr,[49] J. S. Butter,[56] J. Buytaert,[49] W. Byczynski,[49] S. Cadeddu,[32] H. Cai,[75] Y. Cai,[5] A. Caillet,[16] R. Calabrese,[26,g] S. Calderon Ramirez,[9] L. Calefice,[45] S. Cali,[28] M. Calvi,[31,c] M. Calvo Gomez,[46] P. Camargo Magalhaes,[2,i] J. I. Cambon Bouzas,[47] P. Campana,[28] D. H. Campora Perez,[82] A. F. Campoverde Quezada,[7] S. Capelli,[31] L. Capriotti,[26] R. Caravaca-Mora,[9] A. Carbone,[25,j] L. Carcedo Salgado,[47] R. Cardinale,[29,k] A. Cardini,[32] P. Carniti,[31] L. Carus,[22] A. Casais Vidal,[65] R. Caspary,[22] G. Casse,[61] M. Cattaneo,[49] G. Cavallero,[26] V. Cavallini,[26,g] S. Celani,[22] S. Cesare,[30,l] F. Cesario Laterza Lopes,[2] A. J. Chadwick,[61] I. Chahrour,[87] H. Chang,[4,m] M. Charles,[16] Ph. Charpentier,[49] E. Chatzianagnostou,[38] R. Cheaib,[79] M. Chefdeville,[10] C. Chen,[56] J. Chen,[50] S. Chen,[5] Z. Chen,[7] M. Cherif,[12] A. Chernov,[41] S. Chernyshenko,[53] X. Chiotopoulos,[82] V. Chobanova,[84] M. Chrzaszcz,[41] A. Chubykin,[44] V. Chulikov,[28,36] P. Ciambrone,[28] X. Cid Vidal,[47] G. Ciezarek,[49] P. Cifra,[38] P. E. L. Clarke,[59] M. Clemencic,[49] H. V. Cliff,[56] J. Closier,[49] C. Cocha Toapaxi,[22] V. Coco,[49] J. Cogan,[13] E. Cogneras,[11] L. Cojocariu,[43] S. Collaviti,[50] P. Collins,[49] T. Colombo,[49] M. Colonna,[19] A. Comerma-Montells,[45] L. Congedo,[24] J. Connaughton,[57] A. Contu,[32] N. Cooke,[60] C. Coronel,[66] I. Corredoira,[12] A. Correia,[16] G. Corti,[49] J. Cottee Meldrum,[55] B. Couturier,[49] D. C. Craik,[51] M. Cruz Torres,[2,n] E. Curras Rivera,[50] R. Currie,[59] C. L. Da Silva,[68] S. Dadabaev,[44] L. Dai,[72] X. Dai,[4] E. Dall'Occo,[49] J. Dalseno,[84] C. D'Ambrosio,[62] J. Daniel,[11] P. d'Argent,[24] G. Darze,[3] A. Davidson,[57] J. E. Davies,[63] O. De Aguiar Francisco,[63] C. De Angelis,[32,o] F. De Benedetti,[49] J. de Boer,[38] K. De Bruyn,[81] S. De Capua,[63] M. De Cian,[63] U. De Freitas Carneiro Da Graca,[2,p] E. De Lucia,[28] J. M. De Miranda,[2] L. De Paula,[3] M. De Serio,[24,q] P. De Simone,[28] F. De Vellis,[19] J. A. de Vries,[82] F. Debernardis,[24] D. Decamp,[10] S. Dekkers,[1] L. Del Buono,[16] B. Delaney,[65] H.-P. Dembinski,[19] J. Deng,[8] V. Denysenko,[51] O. Deschamps,[11] F. Dettori,[32,o] B. Dey,[79] P. Di Nezza,[28] I. Diachkov,[44] S. Didenko,[44] S. Ding,[69] Y. Ding,[50] L. Dittmann,[22] V. Dobishuk,[53] A. D. Docheva,[60] A. Doheny,[57] C. Dong,[4,m] A. M. Donohoe,[23] F. Dordei,[32] A. C. dos Reis,[2] A. D. Dowling,[69] L. Dreyfus,[13] W. Duan,[73] P. Duda,[83] M. W. Dudek,[41] L. Dufour,[49] V. Duk,[34] P. Durante,[49] M. M. Duras,[83] J. M. Durham,[68] O. D. Durmus,[79] A. Dziurda,[41] A. Dzyuba,[44] S. Easo,[58] E. Eckstein,[18] U. Egede,[1] A. Egorychev,[44] V. Egorychev,[44] S. Eisenhardt,[59] E. Ejopu,[63] L. Eklund,[85] M. Elashri,[66] J. Ellbracht,[19] S. Ely,[62] A. Ene,[43] J. Eschle,[69] S. Esen,[22] T. Evans,[38] F. Fabiano,[32] S. Faghih,[66] L. N. Falcao,[2] B. Fang,[7] R. Fantechi,[35] L. Fantini,[34,r] M. Faria,[50] K. Farmer,[59] D. Fazzini,[31,c] L. Felkowski,[83] M. Feng,[5,7] M. Feo,[19] A. Fernandez Casani,[48] M. Fernandez Gomez,[47] A. D. Fernez,[67] F. Ferrari,[25,j] F. Ferreira Rodrigues,[3] M. Ferrillo,[51] M. Ferro-Luzzi,[49] S. Filippov,[44] R. A. Fini,[24] M. Fiorini,[26,g] M. Firlej,[40] K. L. Fischer,[64] D. S. Fitzgerald,[87] C. Fitzpatrick,[63] T. Fiutowski,[40] F. Fleuret,[15] A. Fomin,[52] M. Fontana,[25] L. F. Foreman,[63] R. Forty,[49] D. Foulds-Holt,[59] V. Franco Lima,[3] M. Franco Sevilla,[67] M. Frank,[49] E. Franzoso,[26,g] G. Frau,[63] C. Frei,[49] D. A. Friday,[63] J. Fu,[7] Q. Führing,[19,56,b] T. Fulghesu,[13] G. Galati,[24] M. D. Galati,[38] A. Gallas Torreira,[47] D. Galli,[25,j] S. Gambetta,[59] M. Gandelman,[3] P. Gandini,[30] B. Ganie,[63] H. Gao,[7] R. Gao,[64] T. Q. Gao,[56] Y. Gao,[8] Y. Gao,[6] Y. Gao,[8] L. M. Garcia Martin,[50] P. Garcia Moreno,[45] J. García Pardiñas,[65] P. Gardner,[67] K. G. Garg,[8] L. Garrido,[45] C. Gaspar,[49] A. Gavrikov,[33] L. L. Gerken,[19] E. Gersabeck,[20] M. Gersabeck,[20] T. Gershon,[57] S. Ghizzo,[29,k] Z. Ghorbanimoghaddam,[55] L. Giambastiani,[33,h] F. I. Giasemis,[16,s] V. Gibson,[56] H. K. Giemza,[42] A. L. Gilman,[64] M. Giovannetti,[28] A. Gioventù,[45] L. Girardey,[63,58] M. A. Giza,[41] F. C. Glaser,[14,22] V. V. Gligorov,[16] C. Göbel,[70] L. Golinka-Bezshyyko,[86] E. Golobardes,[46] D. Golubkov,[44] A. Golutvin,[62,49] S. Gomez Fernandez,[45] W. Gomulka,[40] I. Gonçales Vaz,[49] F. Goncalves Abrantes,[64] M. Goncerz,[41] G. Gong,[4,m] J. A. Gooding,[19] I. V. Gorelov,[44] C. Gotti,[31] E. Govorkova,[65] J. P. Grabowski,[18] L. A. Granado Cardoso,[49] E. Graugés,[45] E. Graverini,[50,t] L. Grazette,[57] G. Graziani,[27] A. T. Grecu,[43] L. M. Greeven,[38] N. A. Grieser,[66] L. Grillo,[60] S. Gromov,[44] C. Gu,[15] M. Guarise,[26] L. Guerry,[11] V. Guliaeva,[44]

P. A. Günther,[22] A.-K. Guseinov,[50] E. Gushchin,[44] Y. Guz,[6,49] T. Gys,[49] K. Habermann,[18] T. Hadavizadeh,[1] C. Hadjivasiliou,[67] G. Haefeli,[50] C. Haen,[49] S. Haken,[56] G. Hallett,[57] P. M. Hamilton,[67] J. Hammerich,[61] Q. Han,[33] X. Han,[22,49] S. Hansmann-Menzemer,[22] L. Hao,[7] N. Harnew,[64] T. H. Harris,[1] M. Hartmann,[14] S. Hashmi,[40] J. He,[7,u] A. Hedes,[63] F. Hemmer,[49] C. Henderson,[66] R. Henderson,[14] R. D. L. Henderson,[1] A. M. Hennequin,[49] K. Hennessy,[61] L. Henry,[50] J. Herd,[62] P. Herrero Gascon,[22] J. Heuel,[17] A. Hicheur,[3] G. Hijano Mendizabal,[51] J. Horswill,[63] R. Hou,[8] Y. Hou,[11] D. C. Houston,[60] N. Howarth,[61] J. Hu,[73] W. Hu,[7] X. Hu,[4,m] W. Hulsbergen,[38] R. J. Hunter,[57] M. Hushchyn,[44] D. Hutchcroft,[61] M. Idzik,[40] D. Ilin,[44] P. Ilten,[66] A. Iniukhin,[44] A. Iohner,[10] A. Ishteev,[44] K. Ivshin,[44] H. Jage,[17] S. J. Jaimes Elles,[77,48,49] S. Jakobsen,[49] E. Jans,[38] B. K. Jashal,[48] A. Jawahery,[67] C. Jayaweera,[54] V. Jevtic,[19] Z. Jia,[16] E. Jiang,[67] X. Jiang,[5,7] Y. Jiang,[7] Y. J. Jiang,[6] E. Jimenez Moya,[9] N. Jindal,[88] M. John,[64] A. John Rubesh Rajan,[23] D. Johnson,[54] C. R. Jones,[56] S. Joshi,[42] B. Jost,[49] J. Juan Castella,[56] N. Jurik,[49] I. Juszczak,[41] D. Kaminaris,[50] S. Kandybei,[52] M. Kane,[59] Y. Kang,[4,m] C. Kar,[11] M. Karacson,[49] A. Kauniskangas,[50] J. W. Kautz,[66] M. K. Kazanecki,[41] F. Keizer,[49] M. Kenzie,[56] T. Ketel,[38] B. Khanji,[69] A. Kharisova,[44] S. Kholodenko,[35,49] G. Khreich,[14] T. Kirn,[17] V. S. Kirsebom,[31,c] O. Kitouni,[65] S. Klaver,[39] N. Kleijne,[35,v] D. K. Klekots,[86] K. Klimaszewski,[42] M. R. Kmiec,[42] S. Koliiev,[53] L. Kolk,[19] A. Konoplyannikov,[6] P. Kopciewicz,[49] P. Koppenburg,[38] A. Korchin,[52] M. Korolev,[44] I. Kostiuk,[38] O. Kot,[53] S. Kotriakhova, E. Kowalczyk,[67] A. Kozachuk,[44] P. Kravchenko,[44] L. Kravchuk,[44] O. Kravcov,[80] M. Kreps,[57] P. Krokovny,[44] W. Krupa,[69] W. Krzemien,[42] O. Kshyvanskyi,[53] S. Kubis,[83] M. Kucharczyk,[41] V. Kudryavtsev,[44] E. Kulikova,[44] A. Kupsc,[85] V. Kushnir,[52] B. Kutsenko,[13] J. Kvapil,[68] I. Kyryllin,[52] D. Lacarrere,[49] P. Laguarta Gonzalez,[45] A. Lai,[32] A. Lampis,[32] D. Lancierini,[62] C. Landesa Gomez,[47] J. J. Lane,[1] G. Lanfranchi,[28] C. Langenbruch,[22] J. Langer,[19] O. Lantwin,[44] T. Latham,[57] F. Lazzari,[35,49,t] C. Lazzeroni,[54] R. Le Gac,[13] H. Lee,[61] R. Lefèvre,[11] A. Leflat,[44] S. Legotin,[44] M. Lehuraux,[57] E. Lemos Cid,[49] O. Leroy,[13] T. Lesiak,[41] E. D. Lesser,[49] B. Leverington,[22] A. Li,[4,m] C. Li,[4] C. Li,[13] H. Li,[73] J. Li,[8] K. Li,[76] L. Li,[63] M. Li,[8] P. Li,[7] P.-R. Li,[74] Q. Li,[5,7] T. Li,[72] T. Li,[73] Y. Li,[8] Y. Li,[5] Y. Li,[4] Z. Lian,[4,m] Q. Liang,[8] X. Liang,[69] Z. Liang,[32] S. Libralon,[48] A. L. Lightbody,[12] C. Lin,[7] T. Lin,[58] R. Lindner,[49] H. Linton,[62] R. Litvinov,[32] D. Liu,[8] F. L. Liu,[1] G. Liu,[73] K. Liu,[74] S. Liu,[5,7] W. Liu,[8] Y. Liu,[59] Y. Liu,[74] Y. L. Liu,[62] G. Loachamin Ordonez,[70] A. Lobo Salvia,[45] A. Loi,[32] T. Long,[56] J. H. Lopes,[3] A. Lopez Huertas,[45] C. Lopez Iribarnegaray,[47] S. López Soliño,[47] Q. Lu,[15] C. Lucarelli,[49] D. Lucchesi,[33,h] M. Lucio Martinez,[48] Y. Luo,[6] A. Lupato,[33,w] E. Luppi,[26,g] K. Lynch,[23] X.-R. Lyu,[7] G. M. Ma,[4,m] S. Maccolini,[19] F. Machefert,[14] F. Maciuc,[43] B. Mack,[69] I. Mackay,[64] L. M. Mackey,[69] L. R. Madhan Mohan,[56] M. J. Madurai,[54] D. Magdalinski,[38] D. Maisuzenko,[44] J. J. Malczewski,[41] S. Malde,[64] L. Malentacca,[49] A. Malinin,[44] T. Maltsev,[44] G. Manca,[32,o] G. Mancinelli,[13] C. Mancuso,[14] R. Manera Escalero,[45] F. M. Manganella,[37] D. Manuzzi,[25] D. Marangotto,[30,l] J. F. Marchand,[10] R. Marchevski,[50] U. Marconi,[25] E. Mariani,[16] S. Mariani,[49] C. Marin Benito,[45] J. Marks,[22] A. M. Marshall,[55] L. Martel,[64] G. Martelli,[34] G. Martellotti,[36] L. Martinazzoli,[49] M. Martinelli,[31,c] D. Martinez Gomez,[81] D. Martinez Santos,[84] F. Martinez Vidal,[48] A. Martorell i Granollers,[46] A. Massafferri,[2] R. Matev,[49] A. Mathad,[49] V. Matiunin,[44] C. Matteuzzi,[69] K. R. Mattioli,[15] A. Mauri,[62] E. Maurice,[15] J. Mauricio,[45] P. Mayencourt,[50] J. Mazorra de Cos,[48] M. Mazurek,[42] M. McCann,[62] T. H. McGrath,[63] N. T. McHugh,[60] A. McNab,[63] R. McNulty,[23] B. Meadows,[66] G. Meier,[19] D. Melnychuk,[42] D. Mendoza Granada,[16] P. Menendez Valdes Perez,[47] F. M. Meng,[4,m] M. Merk,[38,82] A. Merli,[50,30] L. Meyer Garcia,[67] D. Miao,[5,7] H. Miao,[7] M. Mikhasenko,[78] D. A. Milanes,[77,x] A. Minotti,[31,c] E. Minucci,[28] T. Miralles,[11] B. Mitreska,[19] D. S. Mitzel,[19] A. Modak,[58] L. Moeser,[19] R. D. Moise,[17] E. F. Molina Cardenas,[87] T. Mombächer,[49] M. Monk,[57,1] S. Monteil,[11] A. Morcillo Gomez,[47] G. Morello,[28] M. J. Morello,[35,v] M. P. Morgenthaler,[22] J. Moron,[40] W. Morren,[38] A. B. Morris,[49] A. G. Morris,[13] R. Mountain,[69] H. Mu,[4,m] Z. M. Mu,[6] E. Muhammad,[57] F. Muheim,[59] M. Mulder,[81] K. Müller,[51] F. Muñoz-Rojas,[9] R. Murta,[62] V. Mytrochenko,[52] P. Naik,[61] T. Nakada,[50] R. Nandakumar,[58] T. Nanut,[49] I. Nasteva,[3] M. Needham,[59] E. Nekrasova,[44] N. Neri,[30,l] S. Neubert,[18] N. Neufeld,[49] P. Neustroev,[44] J. Nicolini,[49] D. Nicotra,[82] E. M. Niel,[15] N. Nikitin,[44] Q. Niu,[74] P. Nogarolli,[3] P. Nogga,[18] C. Normand,[55] J. Novoa Fernandez,[47] G. Nowak,[66] C. Nunez,[87] H. N. Nur,[60] A. Oblakowska-Mucha,[40] V. Obraztsov,[44] T. Oeser,[17] A. Okhotnikov,[44] O. Okhrimenko,[53] R. Oldeman,[32,o] F. Oliva,[59,49] E. Olivart Pino,[45] M. Olocco,[19] C. J. G. Onderwater,[82] R. H. O'Neil,[49] J. S. Ordonez Soto,[11] D. Osthues,[19] J. M. Otalora Goicochea,[3] P. Owen,[51]

A. Oyanguren,[48] O. Ozcelik,[49] F. Paciolla,[35,y] A. Padee,[42] K. O. Padeken,[18] B. Pagare,[47] T. Pajero,[49] A. Palano,[24] M. Palutan,[28] C. Pan,[75] X. Pan,[4,m] S. Panebianco,[12] G. Panshin,[5] L. Paolucci,[57] A. Papanestis,[58] M. Pappagallo,[24,q] L. L. Pappalardo,[26] C. Pappenheimer,[66] C. Parkes,[63] D. Parmar,[78] B. Passalacqua,[26,g] G. Passaleva,[27] D. Passaro,[35,49,v] A. Pastore,[24] M. Patel,[62] J. Patoc,[64] C. Patrignani,[25,j] A. Paul,[69] C. J. Pawley,[82] A. Pellegrino,[38] J. Peng,[5,7] X. Peng,[74] M. Pepe Altarelli,[28] S. Perazzini,[25] D. Pereima,[44] H. Pereira Da Costa,[68] M. Pereira Martinez,[47] A. Pereiro Castro,[47] C. Perez,[46] P. Perret,[11] A. Perrevoort,[81] A. Perro,[49,13] M. J. Peters,[66] K. Petridis,[55] A. Petrolini,[29,k] J. P. Pfaller,[66] H. Pham,[69] L. Pica,[35,v] M. Piccini,[34] L. Piccolo,[32] B. Pietrzyk,[10] G. Pietrzyk,[14] R. N. Pilato,[61] D. Pinci,[36] F. Pisani,[49] M. Pizzichemi,[31,49,c] V. M. Placinta,[43] M. Plo Casasus,[47] T. Poeschl,[49] F. Polci,[16] M. Poli Lener,[28] A. Poluektov,[13] N. Polukhina,[44] I. Polyakov,[63] E. Polycarpo,[3] S. Ponce,[49] D. Popov,[7,49] S. Poslavskii,[44] K. Prasanth,[59] C. Prouve,[84] D. Provenzano,[32,49,o] V. Pugatch,[53] G. Punzi,[35,t] J. R. Pybus,[68] S. Qasim,[51] Q. Q. Qian,[6] W. Qian,[7] N. Qin,[4,m] S. Qu,[4,m] R. Quagliani,[49] R. I. Rabadan Trejo,[57] R. Racz,[80] J. H. Rademacker,[55] M. Rama,[35] M. Ramírez García,[87] V. Ramos De Oliveira,[70] M. Ramos Pernas,[57] M. S. Rangel,[3] F. Ratnikov,[44] G. Raven,[39] M. Rebollo De Miguel,[48] F. Redi,[30,w] J. Reich,[55] F. Reiss,[20] Z. Ren,[7] P. K. Resmi,[64] M. Ribalda Galvez,[45] R. Ribatti,[50] G. Ricart,[15,12] D. Riccardi,[35,v] S. Ricciardi,[58] K. Richardson,[65] M. Richardson-Slipper,[56] K. Rinnert,[61] P. Robbe,[14,49] G. Robertson,[60] E. Rodrigues,[61] A. Rodriguez Alvarez,[45] E. Rodriguez Fernandez,[47] J. A. Rodriguez Lopez,[77] E. Rodriguez Rodriguez,[49] J. Roensch,[19] A. Rogachev,[44] A. Rogovskiy,[58] D. L. Rolf,[19] P. Roloff,[49] V. Romanovskiy,[66] A. Romero Vidal,[47] G. Romolini,[26,49] F. Ronchetti,[50] T. Rong,[6] M. Rotondo,[28] S. R. Roy,[22] M. S. Rudolph,[69] M. Ruiz Diaz,[22] R. A. Ruiz Fernandez,[47] J. Ruiz Vidal,[82] J. J. Saavedra-Arias,[9] J. J. Saborido Silva,[47] S. E. R. Sacha Emile R.,[49] R. Sadek,[15] N. Sagidova,[44] D. Sahoo,[79] N. Sahoo,[54] B. Saitta,[32,o] M. Salomoni,[31,49,c] I. Sanderswood,[48] R. Santacesaria,[36] C. Santamarina Rios,[47] M. Santimaria,[28] L. Santoro,[2] E. Santovetti,[37] A. Saputi,[26,49] D. Saranin,[44] A. Sarnatskiy,[81] G. Sarpis,[49] M. Sarpis,[80] C. Satriano,[36,z] A. Satta,[37] M. Saur,[74] D. Savrina,[44] H. Sazak,[17] F. Sborzacchi,[49,28] A. Scarabotto,[19] S. Schael,[17] S. Scherl,[61] M. Schiller,[22] H. Schindler,[49] M. Schmelling,[21] B. Schmidt,[49] N. Schmidt,[68] S. Schmitt,[17] H. Schmitz,[18] O. Schneider,[50] A. Schopper,[62] N. Schulte,[19] M. H. Schune,[14] G. Schwering,[17] B. Sciascia,[28] A. Sciuccati,[49] I. Segal,[78] S. Sellam,[47] A. Semennikov,[44] T. Senger,[51] M. Senghi Soares,[39] A. Sergi,[29,k] N. Serra,[51] L. Sestini,[27] A. Seuthe,[19] B. Sevilla Sanjuan,[46] Y. Shang,[6] D. M. Shangase,[87] M. Shapkin,[44] R. S. Sharma,[69] I. Shchemerov,[44] L. Shchutska,[50] T. Shears,[61] L. Shekhtman,[44] Z. Shen,[38] S. Sheng,[5,7] V. Shevchenko,[44] B. Shi,[7] Q. Shi,[7] W. S. Shi,[73] Y. Shimizu,[14] E. Shmanin,[25] R. Shorkin,[44] J. D. Shupperd,[69] R. Silva Coutinho,[69] G. Simi,[33,h] S. Simone,[24,q] M. Singha,[79] N. Skidmore,[57] T. Skwarnicki,[69] M. W. Slater,[54] E. Smith,[65] K. Smith,[68] M. Smith,[62] L. Soares Lavra,[59] M. D. Sokoloff,[66] F. J. P. Soler,[60] A. Solomin,[55] A. Solovev,[44] N. S. Sommerfeld,[18] R. Song,[1] Y. Song,[50] Y. Song,[4,m] Y. S. Song,[6] F. L. Souza De Almeida,[69] B. Souza De Paula,[3] K. M. Sowa,[40] E. Spadaro Norella,[29,k] E. Spedicato,[25] J. G. Speer,[19] P. Spradlin,[60] V. Sriskaran,[49] F. Stagni,[49] M. Stahl,[78] S. Stahl,[49] S. Stanislaus,[64] M. Stefaniak,[88] E. N. Stein,[49] O. Steinkamp,[51] H. Stevens,[19] D. Strekalina,[44] Y. Su,[7] F. Suljik,[64] J. Sun,[32] J. Sun,[63] L. Sun,[75] D. Sundfeld,[2] W. Sutcliffe,[51] V. Svintozelskyi,[48] K. Swientek,[40] F. Swystun,[56] A. Szabelski,[42] T. Szumlak,[40] Y. Tan,[4,m] Y. Tang,[75] Y. T. Tang,[7] M. D. Tat,[22] J. A. Teijeiro Jimenez,[47] A. Terentev,[44] F. Terzuoli,[35,y] F. Teubert,[49] E. Thomas,[49] D. J. D. Thompson,[54] A. R. Thomson-Strong,[59] H. Tilquin,[62] V. Tisserand,[11] S. T'Jampens,[10] M. Tobin,[5,49] T. T. Todorov,[20] L. Tomassetti,[26,g] G. Tonani,[30] X. Tong,[6] T. Tork,[30] D. Torres Machado,[2] L. Toscano,[19] D. Y. Tou,[4,m] C. Trippl,[46] G. Tuci,[22] N. Tuning,[38] L. H. Uecker,[22] A. Ukleja,[40] D. J. Unverzagt,[22] A. Upadhyay,[49] B. Urbach,[59] A. Usachov,[39] A. Ustyuzhanin,[44] U. Uwer,[22] V. Vagnoni,[25] V. Valcarce Cadenas,[47] G. Valenti,[25] N. Valls Canudas,[49] J. van Eldik,[49] H. Van Hecke,[68] E. van Herwijnen,[62] C. B. Van Hulse,[47,aa] R. Van Laak,[50] M. van Veghel,[38] G. Vasquez,[51] R. Vazquez Gomez,[45] P. Vazquez Regueiro,[47] C. Vázquez Sierra,[84] S. Vecchi,[26] J. Velilla Serna,[48] J. J. Velthuis,[55] M. Veltri,[27,bb] A. Venkateswaran,[50] M. Verdoglia,[32] M. Vesterinen,[57] W. Vetens,[69] D. Vico Benet,[64] P. Vidrier Villalba,[45] M. Vieites Diaz,[47] X. Vilasis-Cardona,[46] E. Vilella Figueras,[61] A. Villa,[25] P. Vincent,[16] B. Vivacqua,[3] F. C. Volle,[54] D. vom Bruch,[13] N. Voropaev,[44] K. Vos,[82] C. Vrahas,[59] J. Wagner,[19] J. Walsh,[35] E. J. Walton,[1,57] G. Wan,[6] A. Wang,[7] B. Wang,[5] C. Wang,[22] G. Wang,[8] H. Wang,[74] J. Wang,[6] J. Wang,[5] J. Wang,[4,m] J. Wang,[75] M. Wang,[49] N. W. Wang,[7] R. Wang,[55] X. Wang,[8] X. Wang,[73] X. W. Wang,[62] Y. Wang,[76]

Y. Wang,[6] Y. H. Wang,[74] Z. Wang,[14] Z. Wang,[4,m] Z. Wang,[30] J. A. Ward,[57] M. Waterlaat,[49] N. K. Watson,[54] D. Websdale,[62] Y. Wei,[6] J. Wendel,[84] B. D. C. Westhenry,[55] C. White,[56] M. Whitehead,[60] E. Whiter,[54] A. R. Wiederhold,[63] D. Wiedner,[19] M. A. Wiegertjes,[38] C. Wild,[64] G. Wilkinson,[64,49] M. K. Wilkinson,[66] M. Williams,[65] M. J. Williams,[49] M. R. J. Williams,[59] R. Williams,[56] S. Williams,[55] Z. Williams,[55] F. F. Wilson,[58] M. Winn,[12] W. Wislicki,[42] M. Witek,[41] L. Witola,[19] T. Wolf,[22] E. Wood,[56] G. Wormser,[14] S. A. Wotton,[56] H. Wu,[69] J. Wu,[8] X. Wu,[75] Y. Wu,[6,56] Z. Wu,[7] K. Wyllie,[49] S. Xian,[73] Z. Xiang,[5] Y. Xie,[8] T. X. Xing,[30] A. Xu,[35,v] L. Xu,[4,m] L. Xu,[4,m] M. Xu,[49] Z. Xu,[49] Z. Xu,[7] Z. Xu,[5] K. Yang,[62] X. Yang,[6] Y. Yang,[15] Z. Yang,[6] V. Yeroshenko,[14] H. Yeung,[63] H. Yin,[8] X. Yin,[7] C. Y. Yu,[6] J. Yu,[72] K. Yu,[74] X. Yuan,[5] Y Yuan,[5,7] E. Zaffaroni,[50] J. A. Zamora Saa,[71] M. Zavertyaev,[21] M. Zdybal,[41] F. Zenesini,[25] C. Zeng,[5,7] M. Zeng,[4,m] C. Zhang,[6] D. Zhang,[8] J. Zhang,[7] L. Zhang,[4,m] R. Zhang,[8] S. Zhang,[72] S. Zhang,[64] Y. Zhang,[6] Y. Z. Zhang,[4,m] Z. Zhang,[4,m] Y. Zhao,[22] A. Zhelezov,[22] S. Z. Zheng,[6] X. Z. Zheng,[4,m] Y. Zheng,[7] T. Zhou,[6] X. Zhou,[8] Y. Zhou,[7] V. Zhovkovska,[57] L. Z. Zhu,[7] X. Zhu,[4,m] X. Zhu,[8] Y. Zhu,[17] V. Zhukov,[17] J. Zhuo,[48] Q. Zou,[5,7] D. Zuliani,[33,h] and G. Zunica[50]

(LHCb Collaboration)

[1]*School of Physics and Astronomy, Monash University, Melbourne, Australia*
[2]*Centro Brasileiro de Pesquisas Físicas (CBPF), Rio de Janeiro, Brazil*
[3]*Universidade Federal do Rio de Janeiro (UFRJ), Rio de Janeiro, Brazil*
[4]*Department of Engineering Physics, Tsinghua University, Beijing, China*
[5]*Institute Of High Energy Physics (IHEP), Beijing, China*
[6]*School of Physics State Key Laboratory of Nuclear Physics and Technology, Peking University, Beijing, China*
[7]*University of Chinese Academy of Sciences, Beijing, China*
[8]*Institute of Particle Physics, Central China Normal University, Wuhan, Hubei, China*
[9]*Consejo Nacional de Rectores (CONARE), San Jose, Costa Rica*
[10]*Université Savoie Mont Blanc, CNRS, IN2P3-LAPP, Annecy, France*
[11]*Université Clermont Auvergne, CNRS/IN2P3, LPC, Clermont-Ferrand, France*
[12]*Université Paris-Saclay, Centre d'Etudes de Saclay (CEA), IRFU, Saclay, France, Gif-Sur-Yvette, France*
[13]*Aix Marseille Univ, CNRS/IN2P3, CPPM, Marseille, France*
[14]*Université Paris-Saclay, CNRS/IN2P3, IJCLab, Orsay, France*
[15]*Laboratoire Leprince-Ringuet, CNRS/IN2P3, Ecole Polytechnique, Institut Polytechnique de Paris, Palaiseau, France*
[16]*LPNHE, Sorbonne Université, Paris Diderot Sorbonne Paris Cité, CNRS/IN2P3, Paris, France*
[17]*I. Physikalisches Institut, RWTH Aachen University, Aachen, Germany*
[18]*Universität Bonn - Helmholtz-Institut für Strahlen und Kernphysik, Bonn, Germany*
[19]*Fakultät Physik, Technische Universität Dortmund, Dortmund, Germany*
[20]*Physikalisches Institut, Albert-Ludwigs-Universität Freiburg, Freiburg, Germany*
[21]*Max-Planck-Institut für Kernphysik (MPIK), Heidelberg, Germany*
[22]*Physikalisches Institut, Ruprecht-Karls-Universität Heidelberg, Heidelberg, Germany*
[23]*School of Physics, University College Dublin, Dublin, Ireland*
[24]*INFN Sezione di Bari, Bari, Italy*
[25]*INFN Sezione di Bologna, Bologna, Italy*
[26]*INFN Sezione di Ferrara, Ferrara, Italy*
[27]*INFN Sezione di Firenze, Firenze, Italy*
[28]*INFN Laboratori Nazionali di Frascati, Frascati, Italy*
[29]*INFN Sezione di Genova, Genova, Italy*
[30]*INFN Sezione di Milano, Milano, Italy*
[31]*INFN Sezione di Milano-Bicocca, Milano, Italy*
[32]*INFN Sezione di Cagliari, Monserrato, Italy*
[33]*INFN Sezione di Padova, Padova, Italy*
[34]*INFN Sezione di Perugia, Perugia, Italy*
[35]*INFN Sezione di Pisa, Pisa, Italy*
[36]*INFN Sezione di Roma La Sapienza, Roma, Italy*
[37]*INFN Sezione di Roma Tor Vergata, Roma, Italy*
[38]*Nikhef National Institute for Subatomic Physics, Amsterdam, Netherlands*

[39]Nikhef National Institute for Subatomic Physics and VU University Amsterdam, Amsterdam, Netherlands
[40]AGH - University of Krakow, Faculty of Physics and Applied Computer Science, Kraków, Poland
[41]Henryk Niewodniczanski Institute of Nuclear Physics Polish Academy of Sciences, Kraków, Poland
[42]National Center for Nuclear Research (NCBJ), Warsaw, Poland
[43]Horia Hulubei National Institute of Physics and Nuclear Engineering, Bucharest-Magurele, Romania
[44]Authors affiliated with an institute formerly covered by a cooperation agreement with CERN
[45]ICCUB, Universitat de Barcelona, Barcelona, Spain
[46]La Salle, Universitat Ramon Llull, Barcelona, Spain
[47]Instituto Galego de Física de Altas Enerxías (IGFAE), Universidade de Santiago de Compostela, Santiago de Compostela, Spain
[48]Instituto de Fisica Corpuscular, Centro Mixto Universidad de Valencia - CSIC, Valencia, Spain
[49]European Organization for Nuclear Research (CERN), Geneva, Switzerland
[50]Institute of Physics, Ecole Polytechnique Fédérale de Lausanne (EPFL), Lausanne, Switzerland
[51]Physik-Institut, Universität Zürich, Zürich, Switzerland
[52]NSC Kharkiv Institute of Physics and Technology (NSC KIPT), Kharkiv, Ukraine
[53]Institute for Nuclear Research of the National Academy of Sciences (KINR), Kyiv, Ukraine
[54]School of Physics and Astronomy, University of Birmingham, Birmingham, United Kingdom
[55]H.H. Wills Physics Laboratory, University of Bristol, Bristol, United Kingdom
[56]Cavendish Laboratory, University of Cambridge, Cambridge, United Kingdom
[57]Department of Physics, University of Warwick, Coventry, United Kingdom
[58]STFC Rutherford Appleton Laboratory, Didcot, United Kingdom
[59]School of Physics and Astronomy, University of Edinburgh, Edinburgh, United Kingdom
[60]School of Physics and Astronomy, University of Glasgow, Glasgow, United Kingdom
[61]Oliver Lodge Laboratory, University of Liverpool, Liverpool, United Kingdom
[62]Imperial College London, London, United Kingdom
[63]Department of Physics and Astronomy, University of Manchester, Manchester, United Kingdom
[64]Department of Physics, University of Oxford, Oxford, United Kingdom
[65]Massachusetts Institute of Technology, Cambridge, Massachusetts, USA
[66]University of Cincinnati, Cincinnati, Ohio, USA
[67]University of Maryland, College Park, Maryland, USA
[68]Los Alamos National Laboratory (LANL), Los Alamos, New Mexico, USA
[69]Syracuse University, Syracuse, New York, USA
[70]Pontifícia Universidade Católica do Rio de Janeiro (PUC-Rio), Rio de Janeiro, Brazil (associated with Universidade Federal do Rio de Janeiro (UFRJ), Rio de Janeiro, Brazil)
[71]Universidad Andres Bello, Santiago, Chile (associated with Physik-Institut, Universität Zürich, Zürich, Switzerland)
[72]School of Physics and Electronics, Hunan University, Changsha City, China (associated with Institute of Particle Physics, Central China Normal University, Wuhan, Hubei, China)
[73]Guangdong Provincial Key Laboratory of Nuclear Science, Guangdong-Hong Kong Joint Laboratory of Quantum Matter, Institute of Quantum Matter, South China Normal University, Guangzhou, China (associated with Department of Engineering Physics, Tsinghua University, Beijing, China)
[74]Lanzhou University, Lanzhou, China (associated with Institute Of High Energy Physics (IHEP), Beijing, China)
[75]School of Physics and Technology, Wuhan University, Wuhan, China (associated with Department of Engineering Physics, Tsinghua University, Beijing, China)
[76]Henan Normal University, Xinxiang, China (associated with Institute of Particle Physics, Central China Normal University, Wuhan, Hubei, China)
[77]Departamento de Fisica, Universidad Nacional de Colombia, Bogota, Colombia (associated with LPNHE, Sorbonne Université, Paris Diderot Sorbonne Paris Cité, CNRS/IN2P3, Paris, France)
[78]Ruhr Universitaet Bochum, Fakultaet f. Physik und Astronomie, Bochum, Germany (associated with Fakultät Physik, Technische Universität Dortmund, Dortmund, Germany)
[79]Eotvos Lorand University, Budapest, Hungary (associated with European Organization for Nuclear Research (CERN), Geneva, Switzerland)
[80]Faculty of Physics, Vilnius University, Vilnius, Lithuania (associated with Physikalisches Institut, Albert-Ludwigs-Universität Freiburg, Freiburg, Germany)
[81]Van Swinderen Institute, University of Groningen, Groningen, Netherlands (associated with Nikhef National Institute for Subatomic Physics, Amsterdam, Netherlands)
[82]Universiteit Maastricht, Maastricht, Netherlands (associated with Nikhef National Institute for Subatomic Physics, Amsterdam, Netherlands)

[83]*Tadeusz Kosciuszko Cracow University of Technology, Cracow, Poland (associated with Henryk Niewodniczanski Institute of Nuclear Physics Polish Academy of Sciences, Kraków, Poland)*
[84]*Universidade da Coruña, A Coruña, Spain (associated with La Salle, Universitat Ramon Llull, Barcelona, Spain)*
[85]*Department of Physics and Astronomy, Uppsala University, Uppsala, Sweden (associated with School of Physics and Astronomy, University of Glasgow, Glasgow, United Kingdom)*
[86]*Taras Schevchenko University of Kyiv, Faculty of Physics, Kyiv, Ukraine (associated with Université Paris-Saclay, CNRS/IN2P3, IJCLab, Orsay, France)*
[87]*University of Michigan, Ann Arbor, Michigan, USA (associated with Syracuse University, Syracuse, New York, USA)*
[88]*Ohio State University, Columbus, USA (associated with Los Alamos National Laboratory (LANL), Los Alamos, New Mexico, USA)*

[a]Deceased.
[b]Also at Lamarr Institute for Machine Learning and Artificial Intelligence, Dortmund, Germany.
[c]Also at Università degli Studi di Milano-Bicocca, Milano, Italy.
[d]Also at Università di Roma Tor Vergata, Roma, Italy.
[e]Also at Università di Modena e Reggio Emilia, Modena, Italy.
[f]Also at Department of Physics and Astronomy, University of Victoria, Victoria, Canada.
[g]Also at Università di Ferrara, Ferrara, Italy.
[h]Also at Università di Padova, Padova, Italy.
[i]Also at Universidade Estadual de Campinas (UNICAMP), Campinas, Brazil.
[j]Also at Università di Bologna, Bologna, Italy.
[k]Also at Università di Genova, Genova, Italy.
[l]Also at Università degli Studi di Milano, Milano, Italy.
[m]Also at Center for High Energy Physics, Tsinghua University, Beijing, China.
[n]Also at Universidad Nacional Autónoma de Honduras, Tegucigalpa, Honduras.
[o]Also at Università di Cagliari, Cagliari, Italy.
[p]Also at Centro Federal de Educacão Tecnológica Celso Suckow da Fonseca, Rio De Janeiro, Brazil.
[q]Also at Università di Bari, Bari, Italy.
[r]Also at Università di Perugia, Perugia, Italy.
[s]Also at LIP6, Sorbonne Université, Paris, France.
[t]Also at Università di Pisa, Pisa, Italy.
[u]Also at Hangzhou Institute for Advanced Study, UCAS, Hangzhou, China.
[v]Also at Scuola Normale Superiore, Pisa, Italy.
[w]Also at Università di Bergamo, Bergamo, Italy.
[x]Also at Universidad de Ingeniería y Tecnología (UTEC), Lima, Peru.
[y]Also at Università di Siena, Siena, Italy.
[z]Also at Università della Basilicata, Potenza, Italy.
[aa]Also at Universidad de Alcalá, Alcalá de Henares, Spain.
[bb]Also at Università di Urbino, Urbino, Italy.